*Korean J. Chem. Eng.*, 34(1), 199-205 (2017)
DOI: 10.1007/s11814-016-0227-y

pISSN: 0256-1115
eISSN: 1975-7220

# Parametric studies for $CO_2$ reforming of methane in a membrane reactor as a new $CO_2$ utilization process

**Boreum Lee and Hankwon Lim**†

Department of Advanced Materials and Chemical Engineering, Catholic University of Daegu,
13-13 Hayang-ro, Hayang-eup, Gyeongsan, Gyeongbuk 38430, Korea
(*Received 2 May 2016 • accepted 5 August 2016*)

**Abstract**−A one-dimensional reactor model was employed to perform parametric studies for $CO_2$ reforming of methane in a membrane reactor to investigate its feasibility as a new $CO_2$ utilization process. The effect of key variables such as hydrogen permeance and Ar sweep gas flow rate to facilitate $H_2$ transport from a shell side (retentate) to a tube side (permeate) on the performance in a membrane reactor was studied at various temperatures with numerical simulation validated by experimental results. In addition, increase in $CH_4$ conversion and $H_2$ yield enhancement observed in membrane reactor was successfully confirmed by profiles of $H_2$ partial pressure difference between shell and tube sides. From the numerical simulation studies, the feasibility of using a membrane reactor for $CO_2$ reforming of methane was confirmed by increased $CH_4$ conversion and $H_2$ yield enhancement compared to a packed-bed reactor at the same condition, which in turn leads to significant cost reductions due to a reduced operating temperature. Moreover, a window of $H_2$ permeance and a guideline for Ar sweep gas flow rate for the efficient membrane reactor design was obtained from this study.

Keywords: $CO_2$ Utilization, $CO_2$ Reforming, Membrane Reactor, Hydrogen Permeance, Numerical Simulation

## INTRODUCTION

Reforming reactions with hydrocarbons have been extensively used for the production of a synthesis gas (syngas), an important precursor for various chemicals such as methanol, alkanes, polyethylene, and ethylene glycols [1-3] and hydrogen, a widely used chemical in petrochemical, chemical, and fuel cell sectors. Coupled with high demand for hydrogen and syngas production, a membrane reactor (MR) combining a reactor and a separator together [4] has been applied to various hydrocarbon reforming reactions [5-19] and even water gas shift reaction [20-30] to obtain various advantages over conventional reactors like improved reactant conversions, product yields, and reduced operating costs caused by better performance compared to conventional reactors, to name a few. Due to the technical and economic challenges related to the sequestration of captured $CO_2$, methane dry reforming [31,32], a reaction to convert $CH_4$ and $CO_2$ into hydrogen or syngas, has gained extensive attention as a practical utilization of $CO_2$ captured in various industrial sectors. Various research groups reported their results with regard to the incorporation of a membrane reactor concept into methane dry reforming and confirmed improved reactant conversion and hydrogen yield [33-40]. However, their studies mainly focused on the improved reactant conversion and hydrogen yield with a limited range of reaction conditions and membrane properties. Moreover, even though many works have focused on studies for $CO_2$ reforming of methane in a conventional packed-bed reactor, to our knowledge, little attention has been paid to parametric studies for the effect of a wide range of operating variables and membrane properties on the performance in a membrane reactor from which a practical guideline for an optimized design in a membrane reactor can be sought. In this paper we have investigated the effect of key parameters such as hydrogen permeance, Ar sweep gas flow rate, and operating temperature on the performance in a membrane reactor in terms of $CH_4$ conversion and $H_2$ yield enhancement with correlations of $H_2$ partial pressure difference between shell and tube sides ($P_{H2,\,shell}$-$P_{H2,\,tube}$) in a membrane reactor. From these studies, useful guidelines for the efficient design of a membrane reactor are also presented.

## METHODS

### 1. Model Validation

A one-dimensional reactor modeling, focusing on only single spatial axis, used in the previous studies [30,41-43] has been employed for this study and details are described in Appendix A. The isothermal one-dimension reactor modeling uses differential equations for molar flow rate of each species and incorporates them into reaction rates. Even though only axial direction is considered in this 1-D modeling, it is sufficient enough to provide a preliminary insight to analyze various reactors of interest before fully implementing thorough analysis for concentration and temperature gradients inside reactors. For kinetics used in the modeling, the one proposed by Richardson and Paripatyadar [44] using a $Rh/Al_2O_3$ catalyst was used as shown in Eqs. (1), (2), (3), and (4).

†To whom correspondence should be addressed.
E-mail: hklim@cu.ac.kr
‡This article is dedicated to Prof. Sung Hyun Kim on the occasion of his retirement from Korea University.

The main reactions are $CO_2$ reforming of methane (Eq. (1)) and reverse water gas shift reaction (Eq. (3)), and the corresponding reaction rate expressions in Langmuir-Hinshelwood type were experimentally obtained at atmospheric pressure using a tubular reactor. Numerical simulation studies were performed with assumptions of (a) steady-state operation, (b) negligible heat transfer, (c) negligible radial concentration gradients, and (d) constant hydrogen permeance along the reactor length.

$$CH_4 + CO_2 \rightarrow 2CO + 2H_2 \quad (1)$$

$$r_1 = k_1 * \left[\frac{K_{CO_2} K_{CH_4} P_{CO_2} P_{CH_4}}{(1 + K_{CO_2} P_{CO_2} + K_{CH_4} P_{CH_4})}\right] * \left[1 - \frac{(P_{CO} P_{H_2})^2}{K_1 P_{CH_4} P_{CO_2}}\right] \quad (2)$$

$$CO_2 + H_2 \rightarrow CO + H_2O \quad (3)$$

$$r_2 = K_2 P_{CO_2} \left[1 - \frac{P_{CO} P_{H_2O}}{K_2 P_{CO_2} P_{H_2}}\right] \quad (4)$$

To reflect pressure difference along the reactor in the modeling, Ergun equation [45] as shown in Eqs. (5), (6) and (7) was used in this study.

$$G = \rho v \quad (5)$$

$$\beta_o = \frac{G(1-\phi)}{\rho_o g_c D_p \phi^3}\left[\frac{150(1-\phi)\mu}{D_p} + 1.75G\right] \quad (6)$$

$$\alpha = \frac{2\beta_o}{A_c \rho_c (1-\phi) P_o} \quad (7)$$

To validate the one-dimensional model proposed in this study, we compared numerical results obtained from the modeling to experimental ones obtained from Prabhu et al. [34] at the same reaction conditions. As shown in Fig. 1, numerical results matched well with experimental ones with only slight deviations confirming the validation of our proposed model, and the one-dimensional model was used to carry out parametric studies for key variables, such as hydrogen permeance, Ar sweep gas flow rate, and operating temperature on the performance in a membrane reactor.

### 2. Reaction Conditions and Membrane Properties in a Membrane Reactor

The reaction conditions and physical properties of a membrane used in this study are presented in Table 1. As a reactant mixture, a stream of $CH_4$ and $CO_2$ with a molar ratio of 1 : 1 and Ar as a diluent was fed to a membrane reactor at various operating temperatures from 923 to 1023 K. For a $H_2$ separation membrane, it was assumed that the membrane length was 4.5 cm with a tube diameter of 1.27 cm to represent a lab-scale study. A wide range of $H_2$ permeance from $1\times10^{-9}$ to $2\times10^{-5}$ mol $m^{-2}$ $s^{-1}$ $Pa^{-1}$ was employed for this study to represent different types of inorganic and metallic membranes.

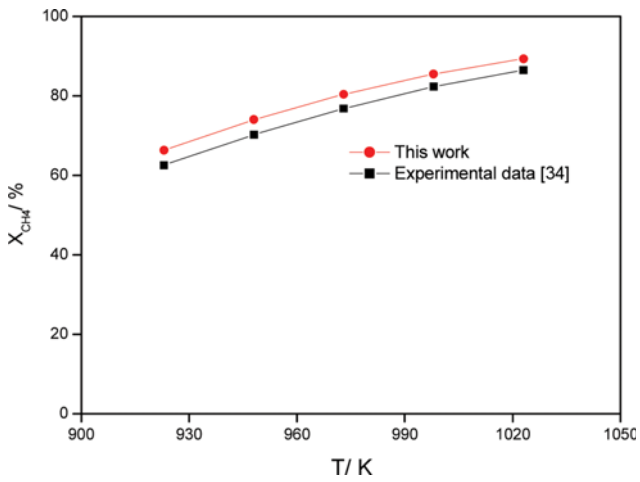


**Fig. 1. Model validation with experimental data.**

**Table 1. Reaction conditions and membrane properties in a membrane reactor**

| | | |
|---|---|---|
| Reactant | $CH_{4\,in}$ (mol $s^{-1}$) | $2.4\times10^{-5}$ |
| | $CH_4 : CO_2$ | 1 : 1 |
| Membrane reactor | T (K) | 923-1023 |
| | Catalyst used (g) | 3.4 |
| | Catalyst diameter (cm) | 0.32 |
| | Void fraction | 0.445 |
| | GHSV* ($h^{-1}$) | 1138 |
| $H_2$ separation membrane | Length (cm) | 4.5 |
| | Tube diameter (cm) | 1.27 |
| | $H_2$ permeance (mol $m^{-2}$ $s^{-1}$ $Pa^{-1}$) | $1\times10^{-9}$-$2\times10^{-5}$ |
| | $H_2$ selectivity | $10^3$ |

*Gas hourly space velocity

## RESULTS AND DISCUSSION

### 1. Effect of $H_2$ Permeance and Ar Sweep Gas on $CH_4$ Conversion in a Membrane Reactor

Fig. 2(a) shows the effect of $H_2$ permeance ($1\times10^{-9}$-$2\times10^{-5}$ mol $m^{-2}$ $s^{-1}Pa^{-1}$) on $CH_4$ conversion in a membrane reactor at 923 K with a fixed $H_2$ selectivity of $10^3$. The $CH_4$ conversion in a packed-bed reactor without membrane (dashed line) was found to be 66.28% from the one-dimensional reactor model simulation. Initially, $CH_4$ conversion in a membrane reactor was similar to one in a packed-bed reactor, but it started to outperform as $H_2$ permeance increased. Thus, there existed a threshold $H_2$ permeance from which a membrane reactor outperformed a packed-bed reactor. These results well demonstrate the importance of $H_2$ permeance as a key factor to derive the extraction of $H_2$ from a shell side to a tube side in a membrane reactor. However, as $H_2$ permeance further increased $CH_4$ conversion reached a plateau for all Ar sweep gas flow rates studied. These phenomena can be explained with further analysis for $H_2$ partial pressure difference between shell and tube sides, denoted as $P_{H2,\,shell}$-$P_{H2,\,tube}$, as shown in Fig. 2(b). This $H_2$ partial pressure difference is regarded as a driving force to derive the extraction of $H_2$ from a shell side to a tube side so that shift of equilibrium to product side can be expected. From Fig. 2(b), it is apparent that the $H_2$ partial pressure difference reaches zero as $H_2$ permeance increases, resulting in no further increase in $CH_4$ conversions in a membrane reactor. From these results, different windows of $H_2$ permeance for different Ar sweep gas flow rates (narrower window for lower $H_2$ permeance: for example, $1\times10^{-8}$-$1\times10^{-6}$ mol $m^{-2}$ $s^{-1}$ $Pa^{-1}$ for Ar sweep gas flow rate of $2.7\times10^{-5}$ mol

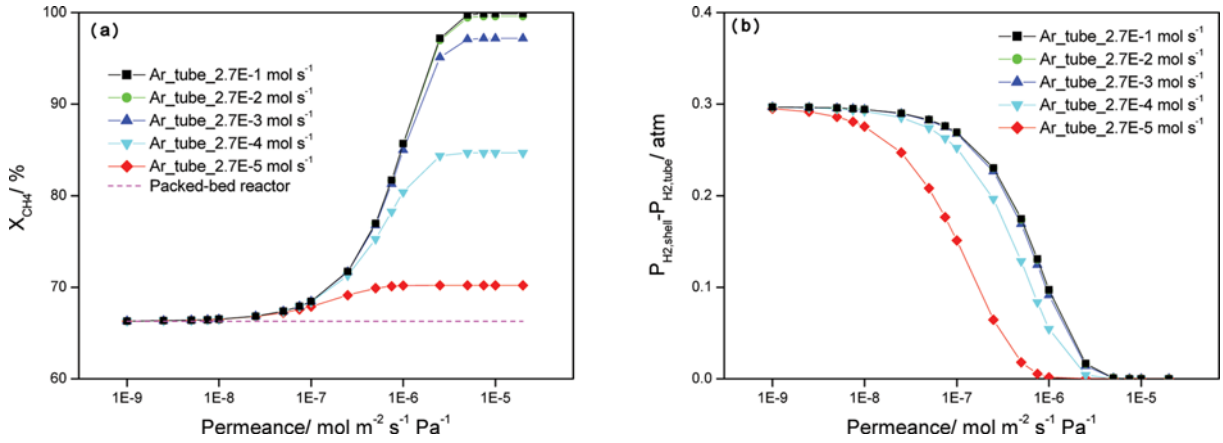


**Fig. 2. Effect of permeance on methane conversion (a) and $H_2$ partial pressure difference (b) with different Ar flow rates at 923 K and $H_2$ selectivity of $10^3$.**

$s^{-1}$ and $1\times10^{-8}$-$5\times10^{-6}$ mol $m^{-2}$ $s^{-1}$ $Pa^{-1}$ for Ar sweep gas flow rate of $2.7\times10^{-1}$ mol $s^{-1}$) can be proposed for the efficient membrane reactor design.

From the studies with Ar sweep gas flow rates, a driving force to derive better sweeping of $H_2$ from a shell side to a tube side, it was apparent that higher Ar sweep gas flow rate was favorable for the $CH_4$ conversions in a membrane reactor. With increased Ar sweep gas flow rate in a tube side of a membrane reactor, higher

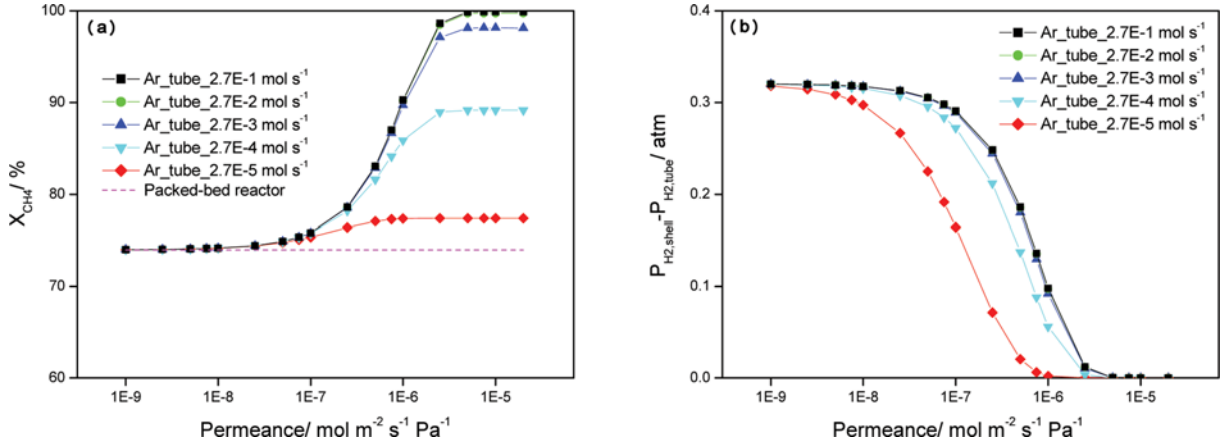


**Fig. 3. Effect of permeance on methane conversion (a) and $H_2$ partial pressure difference (b) with different Ar flow rates at 948 K and $H_2$ selectivity of $10^3$.**

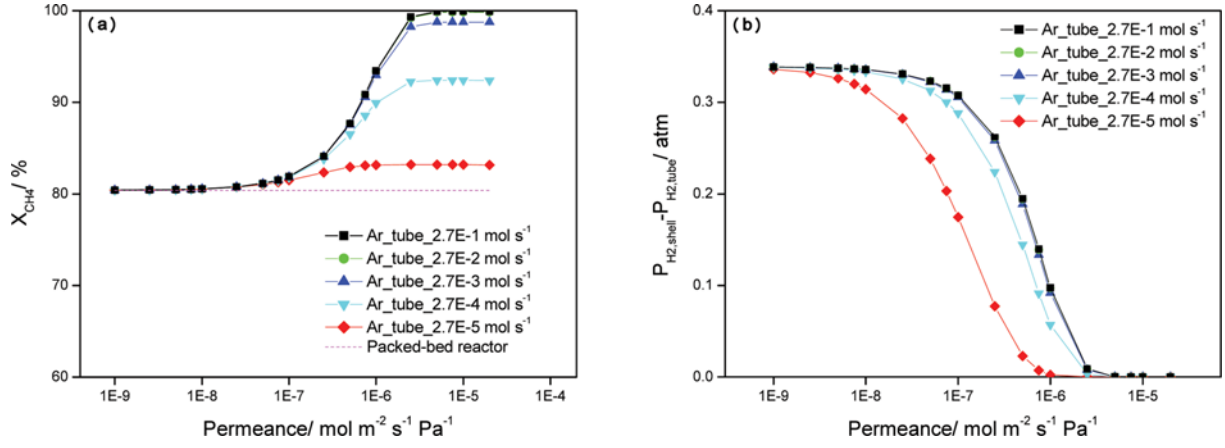


**Fig. 4. Effect of permeance on methane conversion (a) and $H_2$ partial pressure difference (b) with different Ar flow rates at 973 K and $H_2$ selectivity of $10^3$.**

$H_2$ partial pressure difference is clearly shown in Fig. 2(b). At the same time, steeper reduction in $H_2$ partial pressure difference was observed with lower Ar sweep gas flow rate, and it is surmised that this was attributed to the less increased $CH_4$ conversion for lower Ar sweep gas flow as shown in Fig. 2(a). Interestingly, similar $CH_4$ conversions were observed for Ar sweep gas flow rates of $2.7\times10^{-2}$ and $2.7\times10^{-1}$ mol $s^{-1}$ and this can be well explained by the similar $H_2$ partial pressure difference profiles for two cases.

The same analysis was tried for different temperatures of 948 and 973 K and the results are shown in Fig. 3 and 4, respectively. In Fig. 3, the dashed line representing $CH_4$ conversion in a packed-bed reactor of 73.97% at 948 K is shown, and this higher $CH_4$ conversion compared to one at 923 K (66.28%) is consistent with thermodynamic expectation for an endothermic reaction. For a wide range of $H_2$ permeance, higher $CH_4$ conversions than those in a packed-bed reactor were obtained in a membrane reactor after initial thresholds and $H_2$ permeance was favorable for $CH_4$ conversions. In addition, Ar sweep gas flow rate was also favorable for $CH_4$ conversion with no further benefit of Ar sweep gas flow over $2.7\times10^{-2}$ mol $s^{-1}$ again. Less increased $CH_4$ conversions in a mem-

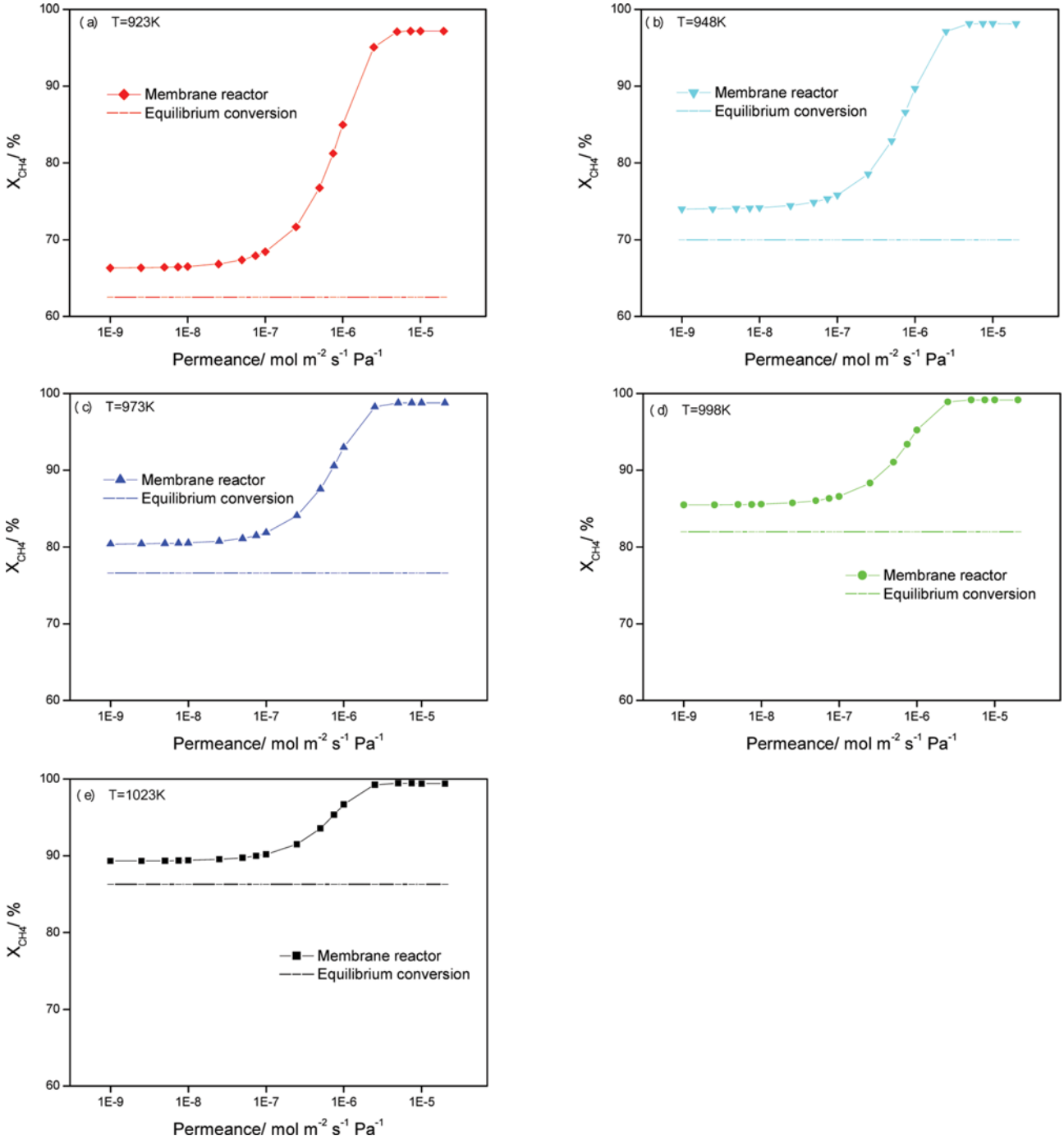


**Fig. 5. Effect of permeance on methane conversion at 923-1023 K with an Ar flow rate of 2.7E-3 mol $s^{-1}$ and $H_2$ selectivity of $10^3$.**

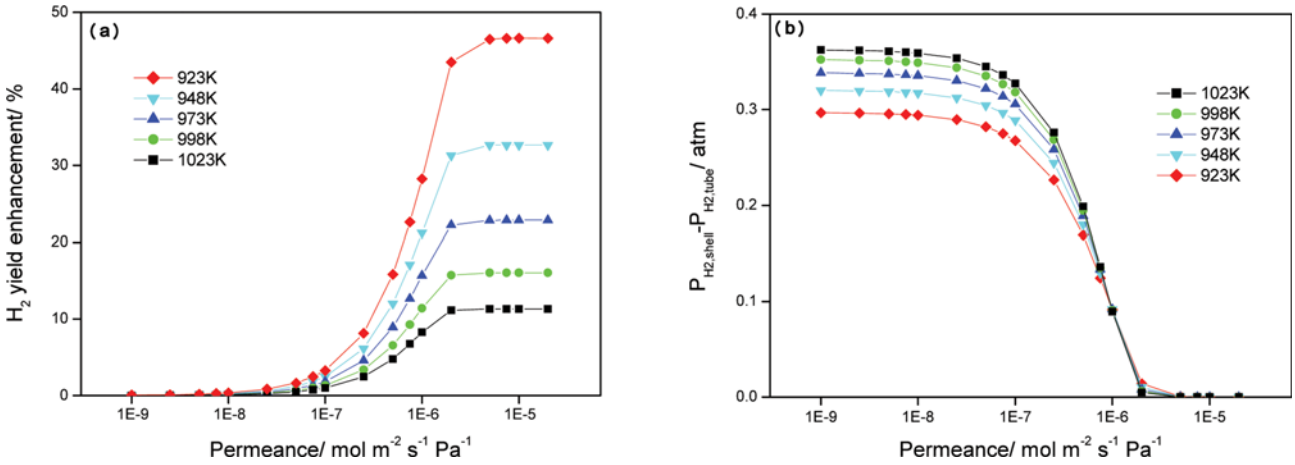


**Fig. 6. Effect of permeance on hydrogen yield enhancement (a) and $H_2$ partial pressure difference (b) at different temperatures with an Ar flow rate of 2.7E-3 mol $s^{-1}$ and $H_2$ selectivity of $10^3$.**

brane reactor with lower Ar sweep gas flow rate can be clearly explained by much steeper reduction in the $H_2$ partial pressure difference in a membrane reactor as shown in Fig. 3(b). Again, there existed a plateau in $CH_4$ conversion for all cases studied and a window of $H_2$ permeance similar with 923 K was also observed for the membrane reactor at 948 K.

Fig. 4 shows a $CH_4$ conversion of 80.39% at 973 K in a packed-bed reactor with a dashed line, and after some initial thresholds higher $CH_4$ conversions in a membrane reactor was also observed. Two important factors, $H_2$ permeance and Ar sweep gas flow, were also favorable for increased $CH_4$ conversion in a membrane reactor, and analysis for $H_2$ partial pressure difference clearly shows the benefit of using a higher Ar sweep gas flow as a driving force in a membrane reactor. Again, a similar window of $H_2$ permeance for an efficient membrane reactor design was observed and no further benefit was obtained for Ar sweep gas flow rates over $2.7\times10^{-2}$ mol $s^{-1}$.

**2. Effect of Temperature on $CH_4$ Conversion and $H_2$ Yield Enhancement in a Membrane Reactor**

To investigate the effect of temperature on $CH_4$ conversion, numerical simulation was carried out for a membrane reactor at temperatures ranging from 923 to 1023 K with a fixed Ar sweep gas flow rate of $2.7\times10^{-3}$ mol $s^{-1}$ and a $H_2$ selectivity of $10^3$. As shown in Fig. 5, $CH_4$ conversion increased as $H_2$ permeance and operating temperature increased. For comparison, equilibrium conversion calculated thermodynamically at each temperature is represented as dashed line [34]. For all conditions studied, better $CH_4$ conversions were obtained in a membrane reactor compared to equilibrium conversion, substantiating the benefit of the membrane reactor due to shift of equilibrium. Note that the effect of operating temperature on $CH_4$ conversion was significant at low $H_2$ permeance, while it was only slight at high $H_2$ permeance. In addition, it was clearly shown that the effect of $H_2$ permeance was negligible when $H_2$ permeance is over about $5\times10^{-6}$ mol $m^{-2}$ $s^{-1}$ $Pa^{-1}$ indicating no further benefit of higher $H_2$ permeance over this value. From this analysis, it can be concluded that a similar trend of increase in $CH_4$ conversion with $H_2$ permeance was observed for all temperatures studied here with significant benefits with lower $H_2$ permeance.

The effect of $H_2$ permeance and operating temperature on $H_2$ yield enhancement, defined as enhanced $H_2$ yield in a membrane reactor compared to a packed-bed reactor, was studied and a clear trend of higher $H_2$ yield enhancement with higher $H_2$ permeance was observed for all temperatures studied, as shown in Fig. 6. As for operating temperatures, higher $H_2$ yield enhancement was obtained with lower operating temperatures. It was also shown that there existed a $H_2$ permeance, over which no further increase in $H_2$ yield enhancement was observed, as supported by $H_2$ partial pressure difference of zero (Fig. 6(b)). This can work as a useful guideline for optimization of some parameters of membranes used in a membrane reactor.

## CONCLUSIONS

A numerical simulation was used for parametric studies for $CO_2$ reforming of methane in a membrane reactor to investigate its feasibility as a new $CO_2$ utilization process. A one-dimensional reactor model was employed and successfully validated by previously reported experimental results. Two important parameters, hydrogen permeance and Ar sweep gas flow rate, considered as a driving for $H_2$ transport through a membrane, were chosen to study the performance in a membrane reactor compared to a packed-bed reactor. It was found from the numerical simulation that both were favorable for $CH_4$ conversion and $H_2$ yield enhancement in a membrane reactor. At the same time, $CH_4$ conversion reached a plateau with increased $H_2$ permeance and a lower $CH_4$ conversion was obtained with a lower Ar sweep flow rate, and these results were successfully explained from the analysis for $H_2$ partial pressure difference between shell and tube sides in a membrane reactor. From the studies with operating temperatures, better $CH_4$ conversion was obtained in a membrane reactor compared to equilibrium conversion. The effect of operating temperature on $CH_4$ conversion was significant at low $H_2$ permeance, while it was only slight at high $H_2$ permeance, and no further increase in $CH_4$ conversion was observed for $H_2$ permeance over about $5\times10^{-6}$ mol $m^{-2}$ $s^{-1}$ $Pa^{-1}$. Also, higher $H_2$ yield enhancement was obtained with lower operating temperature, and it reached a plateau as confirmed by

zero $H_2$ partial pressure difference. The feasibility of using $CO_2$ reforming of methane as a $CO_2$ utilization was confirmed from the simulation results, and it was demonstrated that there existed a window of $H_2$ permeance (for example, $1\times10^{-8}$-$5\times10^{-6}$ mol $m^{-2}$ $s^{-1}$ $Pa^{-1}$ for Ar sweep gas flow rate of $2.7\times10^{-1}$ mol $s^{-1}$) and a guideline for Ar sweep gas flow rate (no further benefit over $2.7\times10^{-2}$ mol $s^{-1}$) for efficient membrane reactor design.

## ACKNOWLEDGEMENTS

This work was supported by research grants from the Catholic University of Daegu in 2015.

## NOMENCLATURE

$F_i$ : molar flow rate of species i on a shell side of a membrane reactor (retentate) [mol $s^{-1}$]
$F_{i,tube}$ : molar flow rate of species i on a tube side of a membrane reactor (permeate) [mol $s^{-1}$]
W : catalyst weight [g]
$k_1$ : rate constant of reaction 1 [mol $g_{cat}^{-1}$ $s^{-1}$]
$k_2$ : rate constant of reaction 2 (mol $atm^{-1}$ $g_{cat}^{-1}$ $s^{-1}$]
$K_{CO_2}$ : adsorption equilibrium constant of $CO_2$ [$Pa^{-1}$]
$K_{CH_4}$ : adsorption equilibrium constant of $CH_4$ [$Pa^{-1}$]
$K_1$ : equilibrium constant for reaction 1 [$Pa^2$]
$K_2$ : equilibrium constant for reaction 2
$r_i$ : reaction rate equation of reaction i [mol $s^{-1}$ $g^{-1}$]
$r_{i,tube}$ : permeation rate equation of species i through a membrane [mol $s^{-1}$ $g^{-1}$]
$K_{H_2,tube}$: proportional constant of $r_{H_2,tube}$ (mol $s^{-1}$ $g^{-1}$ $atm^{-1}$)
P : total pressure on a shell side of a membrane reactor (retentate) [Pa]
$P_o$ : initial pressure at the entrance condition [Pa]
$F_{total}$ : total molar flow rate on a shell side of a membrane reactor (retentate) [mol $s^{-1}$]
$F_o$ : initial total molar flow rate at the entrance condition [mol $s^{-1}$]
$P_i$ : partial pressure of species i on a shell side of a membrane reactor (retentate) [Pa]
$P_{tube}$ : total pressure on a tube side of a membrane reactor (permeate) [Pa]
$F_{total,tube}$: total molar flow rate on a tube side of a MR (permeate) [mol $s^{-1}$]
$P_{i,tube}$ : partial pressure of species i on a tube side of a MR (permeate) [Pa]
$H_{2,permeance}$ : hydrogen permeance [mol $m^{-2}$ $s^{-1}$ $Pa^{-1}$]
$F_{CH_4i}$ : initial molar flow rate of $CH_4$ [mol $s^{-1}$]
$\alpha_i$ : hydrogen selectivity of species i
R : gas constant (8.314 J $mol^{-1}$ $K^{-1}$)
T : reactor temperature [K]
$\phi$ : porosity
$g_c$ : conversion factor [kg m $s^{-2}$ $N^{-1}$]
$D_p$ : diameter of particle in the bed [m]
$\mu$ : viscosity of gas passing through the bed [kg $m^{-1}$ $h^{-1}$]
$\upsilon$ : superficial velocity [m $s^{-1}$]
$\rho$ : gas density [kg $m^{-3}$]
G : superficial mass velocity [kg $m^{-2}$ $s^{-1}$]
$\rho_o$ : gas density of the fluid at the entrance condition [kg $m^{-3}$]
$\rho_c$ : density of the solid catalyst particles [kg $m^{-3}$]
$A_c$ : cross-sectional area [$m^2$]

## REFERENCES

1. J. M. Thomas and W. J. Thomas, *Heterogeneous catalysis,* VCH, Weinheim (1997).
2. M. Seong, M. Shin, J.-H. Cho, Y.-C. Lee, Y.-K. Park and J.-K. Jeon, *Korean J. Chem. Eng.*, **31**, 412 (2014).
3. H.-J. Lee, G. S. Shin and Y.-C. Kim, *Korean J. Chem. Eng.*, **32**, 1267 (2015).
4. J. G. Sanchez Marcano and T. T. Tsotsis, *Catalytic membranes and membrane reactors*, WILEY-VCH, Weinheim (2002).
5. D. Lee, P. Hacarlioglu and S. T. Oyama, *Top. Catal.*, **29**, 45 (2004).
6. S. Irusta, J. Munera, C. Carrara, E. A. Lombardo and L. M. Cornaglia, *Appl. Catal. A: Gen.*, **287**, 147 (2005).
7. T. Tsuru, K. Yamaguchi, T. Yoshioka and M. Asaeda, *AIChE J.*, **50**, 2794 (2004).
8. P. Hacarlioglu, Y. Gu and S. T. Oyama, *J. Nat. Gas Chem.*, **15**, 73 (2006).
9. J. Tong and Y. Matsumura, *Appl. Catal. A: Gen.*, **286**, 226 (2005).
10. C. S. Patil, M. van Sint Annaland and J. A. M. Kuipers, *Chem. Eng. Sci.*, **62**, 2989 (2007).
11. E. Kikuchi, S. Kawabe and M. Matsukata, *J. Jpn. Pet. Inst.*, **46**, 93 (2003).
12. D. Lee, S. Nam, B. Sea, S. Ihm and K. Lee, *Catal. Today*, **118**, 198 (2006).
13. A. Basile, F. Gallucci and L. Paturzo, *Catal. Today*, **104**, 244 (2005).
14. H. Lim, Y. Gu and S. T. Oyama, *J. Membr. Sci.*, **351**, 149 (2010).
15. S. Tosti, A. Basile, F. Borgognoni, V. Capaldo, S. Cordiner, S. Di Cave, F. Gallucci, C. Rizzello, A. Santucci and E. Traversa, *J. Membr. Sci.*, **308**, 250 (2008).
16. S. Vasileiadis, Z. Ziaka and M. Tsimpa, *Int. Trans. J. Eng. Manag. Sci. Technol.*, **2**, 129 (2011).
17. S. Vasileiadis and Z. Ziaka, *Chem. Eng. Sci.*, **59**, 4853 (2004).
18. Z. Ziaka, *Membrane reactors for fuel cells and environmental energy systems*, Xlibris, USA (2009).
19. S. Vasileiadis and Z. Ziaka, *J. Nano Res.*, **12**, 105 (2010).
20. S. Tosti, A. Basile, G. Chiappetta, C. Rizzello and V. Violante, *Chem. Eng. J.*, **93**, 23 (2003).
21. A. Basile, G. Chiappetta, S. Tosti and V. Violante, *Sep. Purif. Technol.*, **25**, 549 (2001).
22. A. Brunetti, G. Barbieri, E. Drioli, K. Lee, B. Sea and D. Lee, *Chem. Eng. Process.*, **46**, 119 (2007).
23. A. Brunetti, A. Caravella, G. Barbieri and E. Drioli, *J. Membr. Sci.*, **306**, 329 (2007).
24. G. Barbieri, A. Brunetti, G. Tricoli and E. Drioli, *J. Power Sources*, **182**, 160 (2008).
25. D. Mendes, V. Chibante, J. Zheng, S. Tosti, F. Borgognoni, A. Mendes and L. M. Madeira, *Int. J. Hydrogen Energy*, **35**, 12596 (2010).
26. D. Mendes, S. Sa, S. Tosti, J. M. Sousa, L. M. Madeira and A. Mendes, *Chem. Eng. Sci.*, **66**, 2356 (2011).
27. Y. Zhang, Z. Wu, Z. Hong, X. Gu and N. Xu, *Chem. Eng. J.*, **197**,

314 (2012).
28. C. A. Cornaglia, S. Tosti, M. Sansovini, J. Munera and E. A. Lombardo, *Appl. Catal. A: Gen.*, **462-463**, 278 (2013).
29. C. A. Cornaglia, M. E. Adrover, J. F. Múnera, M. N. Pedernera, D. O. Borio and E. A. Lombardo, *Int. J. Hydrogen Energy*, **38**, 10485 (2013).
30. H. Lim, *Korean J. Chem. Eng.*, **32**, 1522 (2015).
31. N. Majidian, N. Habibi and M. Rezaei, *Korean J. Chem. Eng.*, **31**, 1162 (2014).
32. N. Rahemi, M. Haghighi, A. A. Babaluo, M. F. Jafari and S. Allahyari, *Korean J. Chem. Eng.*, **31**, 1553 (2014).
33. A. K. Prabhu and S. T. Oyama, *J. Membr. Sci.*, **176**, 233 (2000).
34. A. K. Prabhu, A. Liu, L. G. Lovell and S. T. Oyama, *J. Membr. Sci.*, **177**, 83 (2000).
35. F. Gallucci, S. Tosti and A. Basile, *J. Membr. Sci.*, **317**, 96 (2008).
36. M. L. Bosko, J. F. Munera, E. A. Lombardo and L. M. Cornaglia, *J. Membr. Sci.*, **364**, 17 (2010).
37. J. Li, H. Yoon and E. D. Wachsman, *Int. J. Hydrogen Energy*, **37**, 19125 (2012).
38. F. R. G. Garcia, M. A. Soria, C. Mateos-Pedrero, A. G. Ruiz, I. Rodriguez-Ramos and K. Li, *J. Membr. Sci.*, **435**, 218 (2013).
39. J. Munera, B. Faroldi, E. Frutis, E. Lombardo, L. Cornaglia and S. G. Carrazan, *Appl. Catal. A*, **474**, 114 (2014).
40. S. Sumrunronnasak, S. Tantayanon, S. kiatgamolchai and T. Sukonket, *Int. J. Hydrogen Energy*, **41**, 2621 (2016).
41. S. T. Oyama and H. Lim, *Chem. Eng. J.*, **151**, 351 (2009).
42. H. Lim, *Clean Techol.*, **20**, 425 (2014).
43. A. Alamdari, *J. Nat. Gas Sci. Eng.*, **27**, 934 (2015).
44. J. T. Richardson and S. A. Paripatyadar, *Appl. Catal.*, **61**, 293 (1990).
45. H. S. Fogler, *Essentials of Chemical Reaction Engineering*, Pearson Education, Inc., New Jersey (2010).

## APPENDIX A. ONE-DIMENSIONAL REACTOR MODEL

$$\frac{d(F_{CH_4})}{dW} = -r_1 - r_{CH_4,\,tube}$$

$$\frac{d(F_{CO_2})}{dW} = -r_1 - r_2 - r_{CO_2,\,tube}$$

$$\frac{d(F_{CO})}{dW} = 2 * r_1 + r_2 - r_{CO,\,tube}$$

$$\frac{d(F_{H_2})}{dW} = 2 * r_1 - r_2 - r_{H_2,\,tube}$$

$$\frac{d(F_{H_2O})}{dW} = r_2 - r_{H_2O,\,tube}$$

$$\frac{d(F_{i,\,tube})}{dW} = r_{i,\,tube}$$

$$\frac{d(P/P_o)}{dW} = -\frac{\alpha}{2y} * \frac{F_{total}}{F_o}$$

$$k_1 = 1290 * \exp\left(\frac{-102065}{RT}\right)$$

$$k_2 = (1.856 * 10^{-5}) * \exp\left(\frac{-73105}{RT}\right)$$

$$K_{CO_2} = (2.64 * 10^3) * \exp\left(\frac{37641}{RT}\right)$$

$$K_{CH_4} = (2.63 * 10^3) * \exp\left(\frac{40684}{RT}\right)$$

$$K_1 = (5.9 * 10^{14}) * \exp\left(\frac{-258598.7}{RT}\right)$$

$$K_2 = 68.6829 * \exp\left(\frac{-37500.3}{RT}\right)$$

$$P_i = \frac{F_i}{F_{total}} * P$$

$$P_{i,\,tube} = \frac{F_{i,\,tube}}{F_{total,\,tube}} * P_{tube}$$

$$K_{H_2,\,tube} = \frac{H_{2,\,permeance} * \text{Membrane Area} * (1.01325 * 10^5)}{\text{Weight}}$$

$$r_{H_2,\,tube} = \frac{K_{H_2,\,tube}}{\alpha_i} * (P_{H_2} - P_{H_2,\,tube})$$

$$\text{Conversion} = \frac{(F_{CH4i} - F_{CH_4} - F_{CH_4,\,tube})}{F_{CH4i}}$$